Pavanello, A.; Gomez-Mendoza, M.; De La Peña O'shea, V.; Miranda Alonso, MÁ.; Marín García, ML. (2022). Degradation of Benzotriazole UV-stabilizers in the presence of organic photosensitizers and visible light: A time-resolved mechanistic study. Journal of Photochemistry and Photobiology B Biology. 230:1-11. https://doi.org/10.1016/j.jphotobiol.2022.112444

Degradation of Benzotriazole UV-Stabilizers in the Presence of Organic Photosensitizers and Visible Light: A Time-Resolved Mechanistic Study

Alice Pavanello[1], Miguel Gomez-Mendoza[2], Víctor A. de la Peña O'Shea[2], Miguel A. Miranda[1], M. Luisa Marin[1]*

[1]Instituto de Tecnología Química, Universitat Politècnica de València-Consejo Superior de Investigaciones Científicas, Avda. de los Naranjos s/n, E-46022, Valencia, Spain

[2]Photoactivated Processes Unit, IMDEA Energy Institute, Technological Park of Móstoles, Avda. Ramón de la Sagra 3, 28935 Madrid, Spain

*Corresponding author

E-mail address: marmarin@qim.upv.es

Abstract

Benzotriazole UV-stabilizers (BUVSs) are commonly used in industry as solar filters, due to their strong UV light absorption. Because of their extended usage, environmental contamination of waters due to BUVSs constitutes a growing concern. Direct photodegradation of BUVSs is not efficient due to their intrinsic thermal pathways to release the absorbed light. Nevertheless, their abatement in natural environments could be assisted by chromophoric dissolved organic matter. Among the BUVSs, three representative candidates were selected, UV-326, UV-327 and UV-328, to demonstrate the potential of Riboflavin (RF) as a natural visible-light absorbing photocatalyst for the abatement of these recalcitrant pollutants under reductive conditions. The use of visible light and DABCO, as a model sacrificial electron donor, generates the radical anion $RFTA^{\cdot -}$. This key species reacts with the solar filters, achieving their reductive abatement from the medium. Moreover, the participation of every potential reactive species has been investigated by photophysical techniques, together with determination of the quenching rate constant for every reaction pathway. Consequently, evidence supported the main role of the reductive photodegradation pathway, being $RFTA^{\cdot -}$ the key species in the abatement of BUVSs.

Graphical abstract

Keywords

Advanced Reduction Processes (ARPs), Excited states, Organic matter, Solar filters, Visible light

Highlights

- Tetraacetylated riboflavin (RFTA) acts as a visible light photosensitizer.
- Complex systems were evaluated to determine the best photodegradation conditions.
- RFTA could be used not only for the oxidation but also for the reduction of BUVSs.
- Photoreductive conditions are the most performing ones in the removal of BUVSs.
- Photophysical experiments demonstrate the involvement of $RFTA^{\cdot-}$ in the degradation.

1. Introduction

Benzotriazoles belong to a vast family of chemicals with a variety of industrial applications.[1–3] They exhibit a common heterocyclic structure based on a benzene condensed with a five-membered ring containing three nitrogens. Among them, those having a phenolic substituent at the central nitrogen of the benzotriazole structure absorb strongly UV-A and UV-B light (320-400 and 280-320 nm, respectively) and are thus known as benzotriazole UV-stabilizers (BUVSs) (Figure 1). As a result, BUVSs are frequently used as additives to protect from yellowing and light-induced degradation of products such as building materials, auto components, paints or polymeric materials, as well as in toiletry formulations (soaps, shampoos, foams, lotions, creams, sunscreens).[3–5] In fact, BUVSs such as UV-234, UV-328 and UV-329 are currently listed as High Production Volume Chemicals (HPVC).[6]

Because of their widespread usage, BUVSs easily enter the environment from inefficient removal in wastewater treatment plants, or as direct wash-off from human body. Consequently, contamination of aquatic environments, including marine organisms, surface water or indoor habitats, due to BUVSs has become a growing environmental concern.[6–8] For instance, Government of Japan has classified UV-320, as a Class I Specified Chemical Substance and UV-327 as a Monitoring Chemical Substance, because of their potential toxicity, persistence and tendency to bioaccumulation.[9] In this context, the high lipophilicity of BUVSs (log K_{ow} in the range 6.6-8.3) is associated to their adsorption to biomass and could be magnified through the trophic chain.[10] In general, BUVSs do not exhibit estrogen nor androgenic activity, except from UV-P, which shows clear antiandrogenic activity using a yeast two-hybrid assay.[11] More recently, UV-P, UV-9, UV-326 and UV-090 show aryl hydrocarbon receptor agonistic activity, therefore they constitute a potential risk to human health.[12] With this background, there is a need to face the degradation of this family of contaminants. Direct photodegradation of BUVSs is not efficient enough due to their intrinsic thermal pathways to release the absorbed light.

Examples of recent technologies that have emerged for photocatalytic water treatment include metal-organic frameworks [13,14], aluminosilicates[15], inorganic-organic composites based on metal oxides [16,17] and biochar-based catalysts [18]. Biochar and the aluminosilicates such as kaolinite and montmorillonite, loaded with inorganic semiconductor photocatalysts have been widely applied in photocatalysis by adsorptional-photocatalytic removal protocols. On the other hand, MOFs exhibit crystallinity, large surface areas, adsorption performance, stability and component tunability. Unfortunately, despite the great advantages of MOFs, there are some limitations, including: (i) the nanoscale size of powdered MOF induces aggregation triggering blocking troubles in water treatment; (ii) synthesis of MOFs with controllable size/shape is complex and costly, and not applicable to a large-scale production.[19,20]

Nevertheless, the abatement of BUVSs in natural environments could be assisted by chromophoric dissolved organic matter (CDOM). Upon solar irradiation, CDOM produces ^{1}CDOM* that through intersystem crossing gives ^{3}CDOM*, which could directly react with BUVSs or could react with O_2 or inorganic salts to generate further reactive species. The variety of excited states and reactive intermediates with different energies and redox potentials make CDOM an attractive alternative to address photodegradation of organic pollutants as well as very challenging due to its complexity.[21] However, this approach has only been employed for the removal of UV-P, using CDOMs from different sources and selective chemical probes.[22] The obtained results indicate that the pathways involving hydroxyl radical or singlet oxygen are not significant in the CDOM-mediated photodegradation of UV-P, while the triplet excited state ^{3}CDOM* plays the dominant role.

For this reason, it seems appealing to explore the behavior of BUVSs in the presence of naturally occurring photosensitizers as models for CDOM. In this context, Riboflavin (RF), the natural soluble vitamin B_2, is commonly found as an ingredient of CDOM in natural aqueous systems. It absorbs UV-visible light, and subsequently can produce the abatement of a variety of pollutants through oxidative mechanisms.[23–25] Its photophysical properties, including the energy of its first singlet and triplet excited states, and redox potentials

have been fully characterized.[26–31] Thus, RF is deemed to be one of the most probable photosensitizers to explain the "natural" degradation of pollutants under environmental conditions.[32–36] Moreover, RF could also participate in the photoreduction of model halogenated organic compounds in the presence of suitable electron donors.[37] Actually, Advanced Reduction Processes (ARPs) are emerging as suitable techniques to generate reactive radicals with a remarkable reductive capability.[38,39] A deep understanding on the role of naturally occurring constituents of the environment in the photodegradation of pollutants could constitute an step forward to a more sustainable wastewater remediation.

With this background, the aim of the present work is to investigate the feasibility of using an organic photosensitizer, such as RF, alone or upon addition of a sacrificial electron donor, as a proxy of CDOM to achieve the photodegradation of a variety of BUVSs. Moreover, a systematic investigation on the kinetic behavior of the different excited states and reactive species involved would allow postulating a plausible mechanism to explain such photodegradations. To enhance the prospects of RF, it was derivatized upon transformation in the tetraacetylated riboflavin (RFTA).[40] Among the BUVSs, three representative candidates were selected, UV-326, UV-327 and UV-328, to demonstrate the potential of RF as a natural photosensitizer for the abatement of these recalcitrant pollutants under different scenarios (Figure 1).

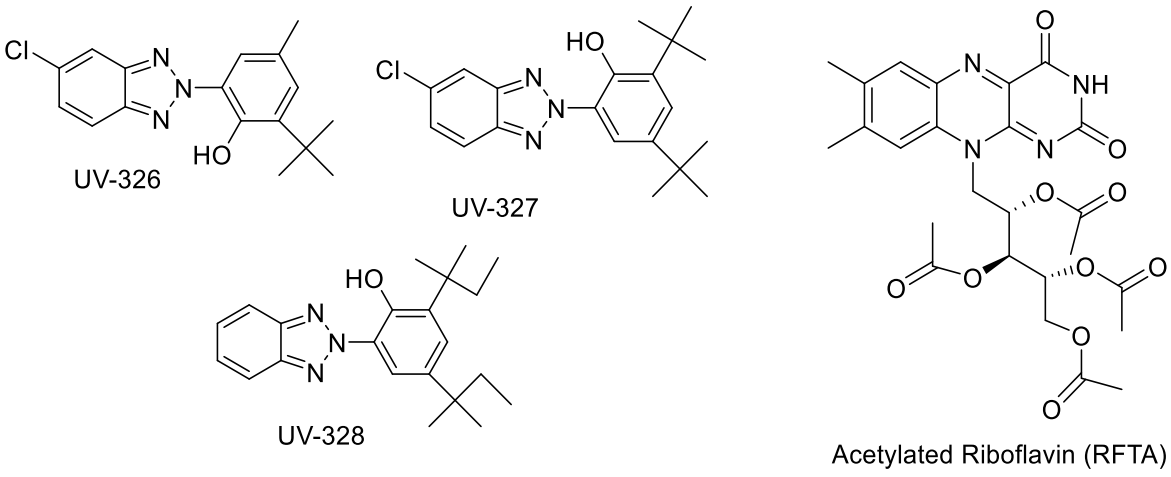

Figure 1. Selected Benzotriazole-UV stabilizers (BUVSs) and acetylated riboflavin (RFTA) employed in this work.

2. Experimental

2.1. Chemicals

UV-326 (2-(2'-hydroxy-3'-*tert*-butyl-5'-methylphenyl)-5-chloro-2*H*-benzotriazole, CAS 3896-11-5); UV-327 (2-(2'-hydroxy-3',5'-di-*tert*-butylphenyl)-5-chloro-2*H*-benzotriazole, CAS 3864-99-1); UV-328 (2-(2'-hydroxy-3',5'-di-*tert*-amylphenyl)-2*H*-benzotriazole, CAS 25973-55-1), Rose Bengal and Riboflavin were from TCI Chemicals. Dimethylsulfoxide (DMSO), dimethylformamide (DMF), acetonitrile and toluene were

from Scharlau. Acetylated riboflavin was synthetized according to a previously reported procedure.[40] Milli-Q water was always employed. All reagents (analytical grade) were used as received.

2.2. Photodegradations

Mother solutions of each contaminant ($1x10^{-3}$ M in DMF), acetylated riboflavin ($1x10^{-3}$ M in acetonitrile). And DABCO (1,4-diazabicyclo[2.2.2]octane) ($2x10^{-1}$ M in Milli-Q water) were first prepared. Then, photodegradations were run in 25 mL of aqueous solutions containing the pollutant (10^{-5} M), RFTA (10^{-6} M, 10% mol) and DABCO (10^{-2} M) when specified, upon irradiation in test tubes using a homemade LED photoreactor (λ_{max} = 450 nm) under the specified atmosphere. To monitor the progress of the photodegradations, aliquots of 0.5 mL were sampled and analyzed by HPLC-UV; the details of the setup can be found elsewhere.[24,37] Elution was performed with an acetonitrile/water mixture (90:10, v:v) at pH 3, in the isocratic mode, and the flow rate was 1.5 mL min^{-1}. The samples were analyzed at 350 nm. Calibration lines were used to determine the concentrations. Experiments were carried out in triplicate.

2.3 Photophysical experiments

UV visible spectra

For recording the UV visible spectra an Agilent Cary 50 spectrophotometer was employed. Mother solutions of each contaminant in DMSO ($1x10^{-3}$ M) were diluted down to 5 x 10^{-5} M in the indicated solvent and placed in quartz cuvettes with an optical path of 1 cm. Obtained absorbance were divided by the concentration to get the spectra as molar absorption coefficient *versus* wavelength (Figure S1).

Steady-state and time-resolved fluorescence

Emission experiments were performed either with a FLS1000 (Edinburgh instruments) spectrofluorometer, for steady state experiments, or with an EasyLife V (OBB) instrument, for lifetime measurements. Steady-state measurements were carried out exciting at λ_{exc} = 445 nm, the emission was registered from 460 nm to 700 nm. Time-resolved fluorescence was measured upon excitation with a LED diode (λ_{exc} = 460 nm) and using a cut-off filter (50 % transmission at 475 nm) (Figure S2).

Typically, quenching experiments were run by adding increasing volumes of fresh solutions of UV-326, UV-327 or UV-328 in toluene to the RFTA solution (absorbance 0.15 at the excitation wavelength) in aerated acetonitrile.

Transient absorption (Laser Flash Photolysis)

Laser flash photolysis experiments were carried out using the previously described equipment and procedures[24]. Unless otherwise specified, the selected wavelengths for excitation and monitoring were 460 and 385 nm, respectively. All data were obtained at room temperature using 10 x 10 mm^2 quartz cells, after bubbling with N_2 during 15 min.

Typically, for the quenching experiments, appropriate volumes of fresh solutions of UV-326, UV-327 or UV-328 in toluene (2 mM) were added to the purged RFTA solution (absorbance 0.3 a λ_{exc} = 460 nm) in acetonitrile containing (if specified) 50 mM of DABCO. The prepared solar filter stock solutions contained the same concentration of RFTA in order to avoid a dilution effect.

Singlet oxygen generation was achieved by excitation of a solution of Rose Bengal in aerated acetonitrile (absorbance ca. 0.5 at 532 nm) by means of a Nd:YAG laser. The characteristic emission of $^1O_2$ at 1270 nm was monitored using a Hamamatsu NIR detector. The degree of quenching of this signal was determined by the progressive shortening of its lifetime in the presence of increasing concentrations of solar filters.

2.4 Cyclic Voltamperometry

Cyclic voltammetric experiments were carried out in a VersaSTAT 3 workstation (Princeton Applied Research) using a quartz cell with 3 electrodes: a glassy carbon (GCE) as a working electrode, a Pt electrode as counter electrode and an Ag/AgCl electrode (saturated of KCl) as the reference electrode. Mother solutions of each BUVS were prepared in DMSO at 10^{-2}M and then they were diluted to reach the working concentration (10^{-5} M) in Phosphate Buffer (PB) 0.1M pH 7 as electrolite. The experiments were registered in N_2 atmosphere with a scan rate of 0.05V/s. The values of redox potential were obtained as the average between the minimum and the maximum of the cyclic scan curves. All the obtained data were then converted into standard calomel electrode values E (vs SCE).

3. Results and Discussion

3.1 Photodegradation of BUVSs under different scenarios

With the aim of obtaining the best scenario to produce the photodegradation of the BUVSs, a careful design of photodegradation experiments was planned with increasing levels of complexity.

Initially, photolysis of individual aqueous solutions of the BUVSs was carried out under visible (blue LEDs, λ_{max} 450 nm), and also under UV light (λ_{max} 355 nm). The obtained results are shown in Figure 2. Not surprisingly, the BUVSs resulted to be refractory to the direct irradiation even upon long exposure times, in agreement with their main application as solar filters.

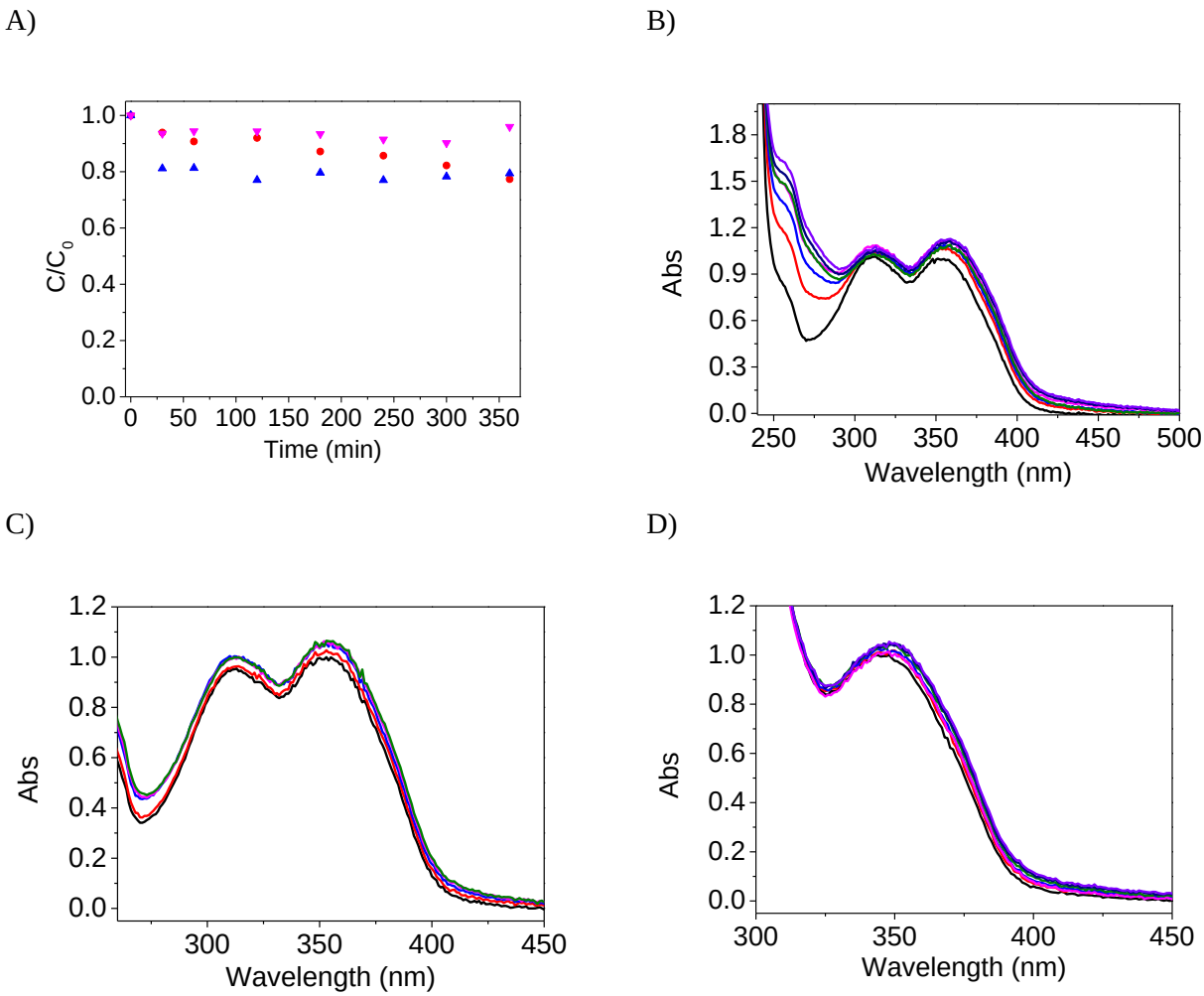

Figure 2. Separate photolysis of aerated aqueous solutions of UV-326 (●), UV-327 (▲) and UV-328 (▼) under blue LED light (λ_{max} = 450 nm), monitored by HPLC (A). Photolysis of UV-326 (B), UV-327 (C) and UV-328 (D) under air, using UVA lamps (λ_{max} = 350 nm), monitored by UV-Vis spectrophotometry up to 3h.

Next, a good electron donor, such as DABCO, was incorporated into the system, and aerated aqueous solutions of each filter plus DABCO were irradiated under UV light. The obtained results are shown in Figure 3. UV-326 experienced a significant photodegradation (see Figure 3A) upon 3h irradiation, while UV-327 and UV-328 were almost unreactive under the same experimental conditions.

Next, the complexity of the system was increased by the presence of RFTA, a natural photosensitizer that could be considered as a good model of CDOM. The effect of RFTA was evaluated upon selective irradiation (using only blue LEDs as irradiation source) under anaerobic and aerobic atmosphere (Figure 4). Again, UV-326 was the most reactive filter achieving ca 30% photodegradation upon 6 h irradiation, while the abatement of the other two was negligible in the absence of O_2 (Figure 4A). It is worth mentioning that the photodegradation extent under aerated conditions reached 60% upon 6 hours of irradiation regardless the chemical structure of BUVSs (Figure 4B). This is in agreement with an initial oxidation of the BUVSs giving rise to the formation of reactive radicals, which in the presence of O_2 are able to initiate chain reactions that

eventually lead to oxidation products more efficiently under aerobic atmosphere. Moreover, it could also indicate oxidation of BUVSs by singlet oxygen generated from the triplet excited state of RFTA.

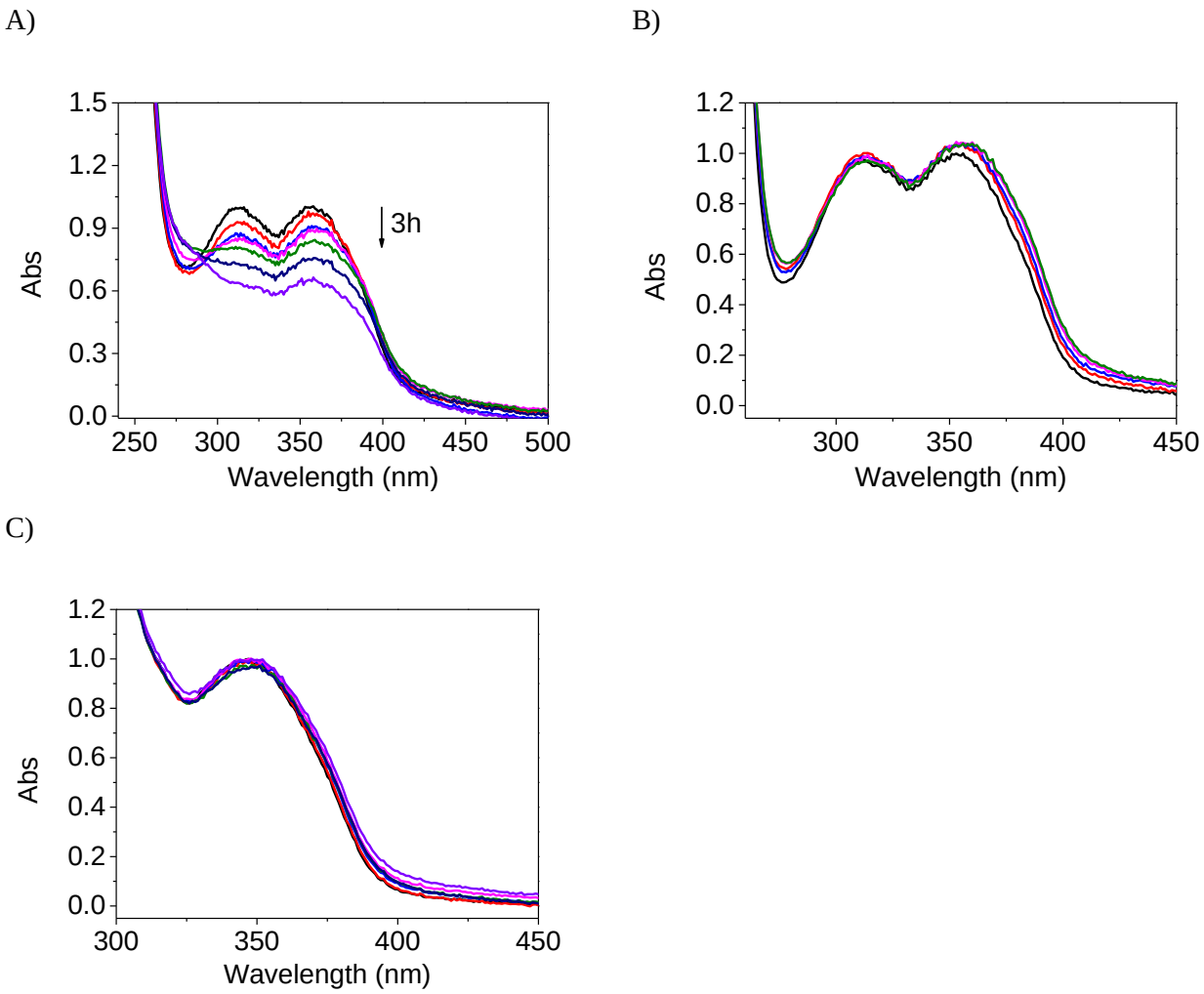

Figure 3. Irradiation of UV-326 (A), UV-327 (B) and UV-328 (C) under UVA lamps (λ_{max}= 350 nm), in the presence of 10^{-2} M DABCO.

Lastly, an even more complex scenario was envisaged, since RFTA could be found simultaneously with good sacrificial electron donors able to generate the corresponding radical anion $RFTA^{\bullet-}$, which could act as a reductant of recalcitrant contaminants. To evaluate this scenario, DABCO was again selected, as it is an efficient quencher of the singlet excited state of RFTA (k_q = 4.5x10^9 $M^{-1}s^{-1}$) giving rise to $RFTA^{\bullet-}$.[37]

Thus, irradiation of the three BUVSs was run after addition of a high concentration of DABCO (10^{-2} M) to ensure a complete reduction of ^{1}RFTA* (Figure 5). Under these conditions, the abatement of the BUVSs was much more efficient than under the previous ones. Specifically, in the absence of air, UV-326 was completely removed in three hours, UV-327 needed 6 hours for complete abatement, and even the more recalcitrant UV-328 was removed, up to 80%, upon 6 hours. More interestingly, under aerobic atmosphere the abatement of the filters was even faster: complete abatement of UV-326 and UV-327 and 70% of UV-328 was achieved only upon 2 hours irradiation. Again, O_2 is able to initiate chain reactions that eventually lead to oxidation

products more efficiently under aerobic atmosphere, although participation of singlet oxygen could not be disregarded.

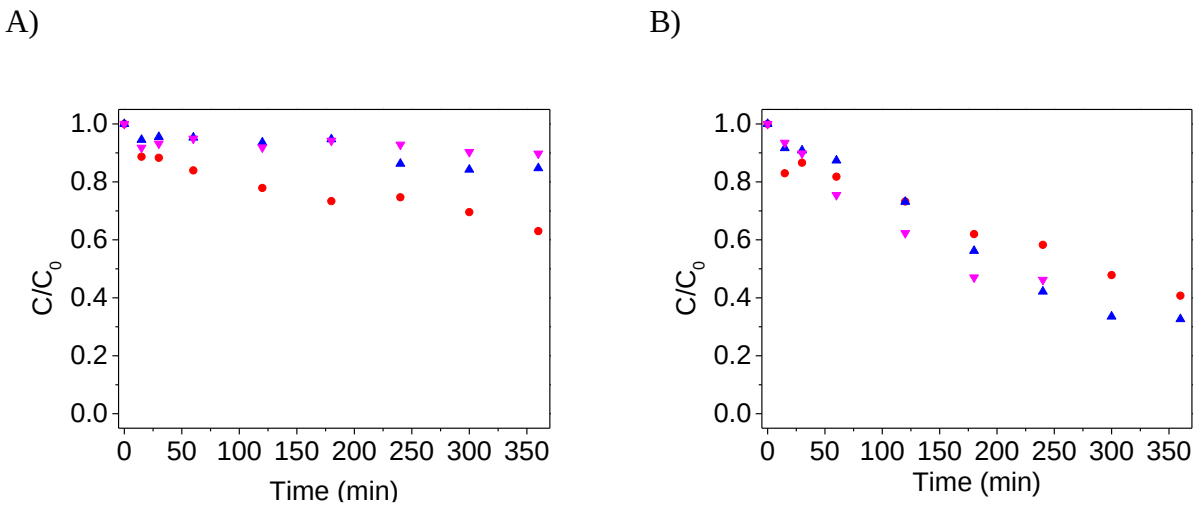

Figure 4. Photodegradation of UV-326 (●), UV-327 (▲) or UV-328 (▼) (10^{-5} M) under a blue LED (λ_{max}= 450 nm) irradiation in the presence of RFTA (10% mol) in N_2 (A) and air (B).

In summary, the best scenario to achieve the abatement of the filters needs the presence of a visible light absorbing photosensitizer, such as RFTA, plus a good e^- donor as DABCO; the presence of O_2 improves the efficiency of the system under all conditions. Natural incomes of vitamin B (RF) could compensate the lack of recyclability of RFTA; thus this fact does not constitute a drawback for photocatalytic wastewater remediation.

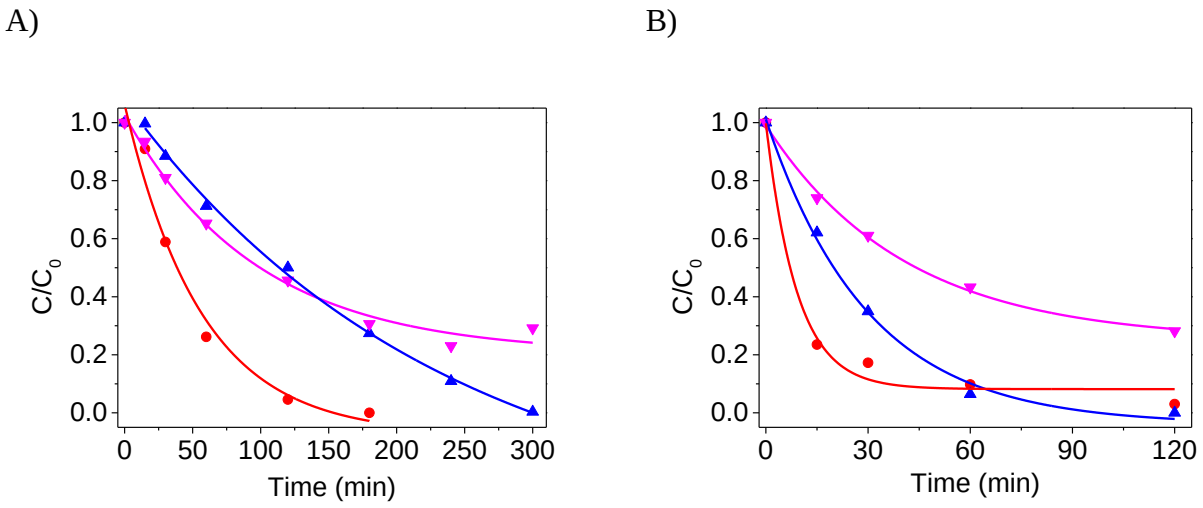

Figure 5. Photocatalytic degradation of aqueous mixtures of UV-326 (●), UV-327 (▲) or UV-328 (▼) (10^{-5} M) in the presence of RFTA (10% mol) and DABCO (10^{-2} M) in N_2 (A) and air (B) using a blue LED as light source (λ_{max}= 450 nm).

3.2 Quenching of the RFTA excited states

Initially, evaluation of the direct participation of singlet and triplet excited states of RFTA was performed in an attempt to understand the photodegradation results.

A)

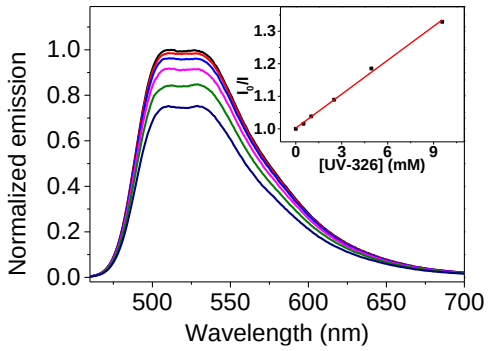

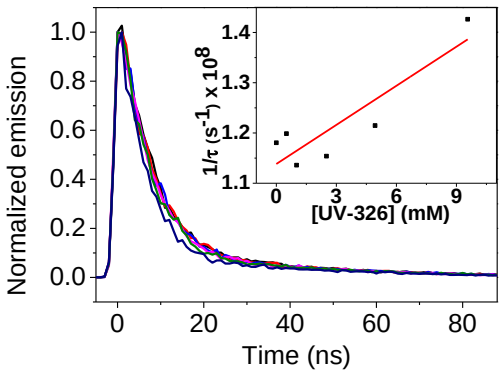

B)

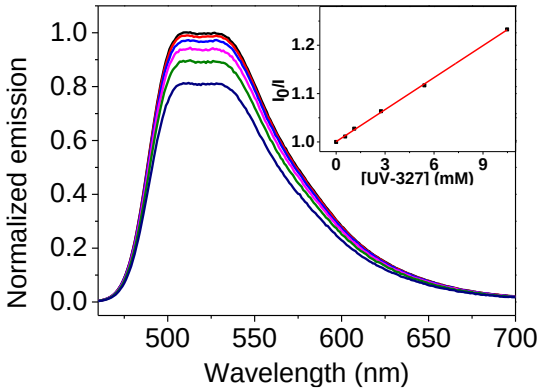

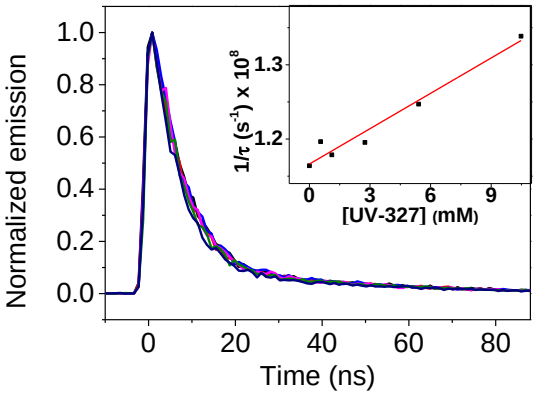

C)

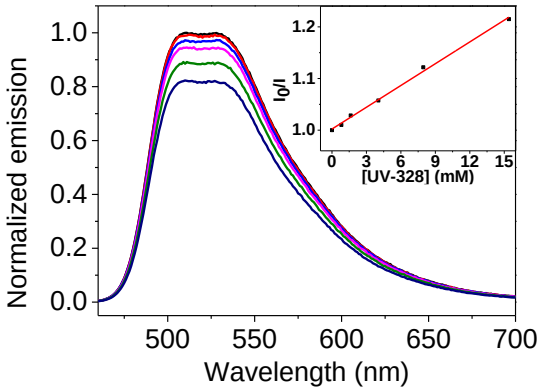

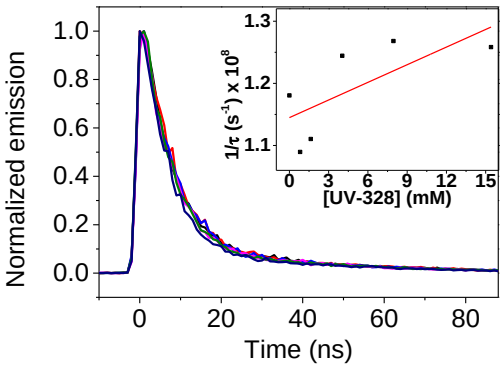

Figure 6. Quenching of the ^{1}RFTA* steady-state (left, λ_{exc} = 445 nm) and time-resolved emission (right, λ_{exc} = 460 nm) by UV-326 (A); UV-327 (B) and UV-328 (C), in aerated CH_3CN.

In fact, steady-state emission of ^{1}RFTA* was quenched by increasing concentrations of the three BUVSs (see Figure 6 left column), with K_{SV} values of 34.8 M^{-1}, 22.1 M^{-1} and 14.0 M^{-1} for UV-326, UV-327 and UV-328, respectively. Even more, time-resolved measurements were also carried out, and the obtained values for the quenching constants were close to diffusion control: k_{qS} = 2.6 x 10^9 $M^{-1}s^{-1}$ and k_{qS} = 1.6 x 10^9 $M^{-1}s^{-1}$ for UV-326 and UV-327, respectively. It should be noted that fitting of the experimental data corresponding to UV-328 was not reliable; in this case, the estimated value of k_{qS} was 9.5 x 10^8 $M^{-1}s^{-1}$.

Emission of ^{1}RFTA* was also recorded upon addition of DABCO, and the obtained quenching rate constant value from the decrease of the singlet lifetime was k_{qS} = 1.2 x 10^{10} $M^{-1}s^{-1}$; close to diffusion control (see Figure 7).[41]

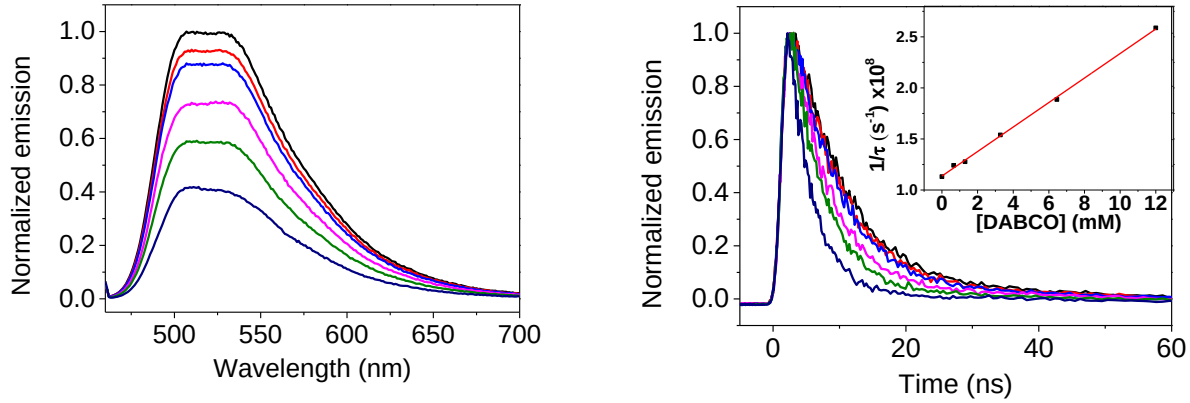

Figure 7. Quenching of the ^{1}RFTA* steady-state (left, λ_{exc} = 445 nm) and time-resolved emission (right, λ_{exc} = 460 nm) by DABCO, in aerated CH_3CN.

Next, laser flash photolysis (LFP) was performed to investigate the participation of ^{3}RFTA* in the photodegradation. For this purpose, deaerated solutions of RFTA (Abs = 0.3 at the λ_{exc} = 460 nm) were photolyzed upon addition of increasing amounts of the BUVSs, showing the characteristic triplet-triplet absorption of RFTA (a peak at 385 nm and a broad band between 500 and 700 nm, Figure 8A). Nevertheless, the decay of the triplet excited state, monitored at 620 nm, remained unchanged upon increasing concentration of the BUVSs (Figures 8B-D), indicating that direct reaction of the BUVSs with ^{3}RFTA* is not involved in the observed photodegradations.

Moreover, although ^{1}RFTA* is efficiently quenched by DABCO, the fraction of non-quenched singlets that arrive into the triplet upon intersystem crossing, could also be quenched by DABCO. To investigate such possibility, deaerated solutions of RFTA (Abs = 0.3 at the λ_{exc} = 460 nm) were treated with different amounts of DABCO. From the observed decrease in the ^{3}RFTA* lifetime, recorded at 620 nm, the obtained quenching constant value was k_{qT} = 7.8 x 10^9 $M^{-1}s^{-1}$ (Figure 9). Moreover, when the experiment was performed in the presence of 50 mM of DABCO, a new species was observed. This species displayed a strong absorption at 380 nm and a less intense one between 470 and 650 nm. This species was assigned to the $RFTA^{\bullet-}$ on the basis of previously reported data.[37]

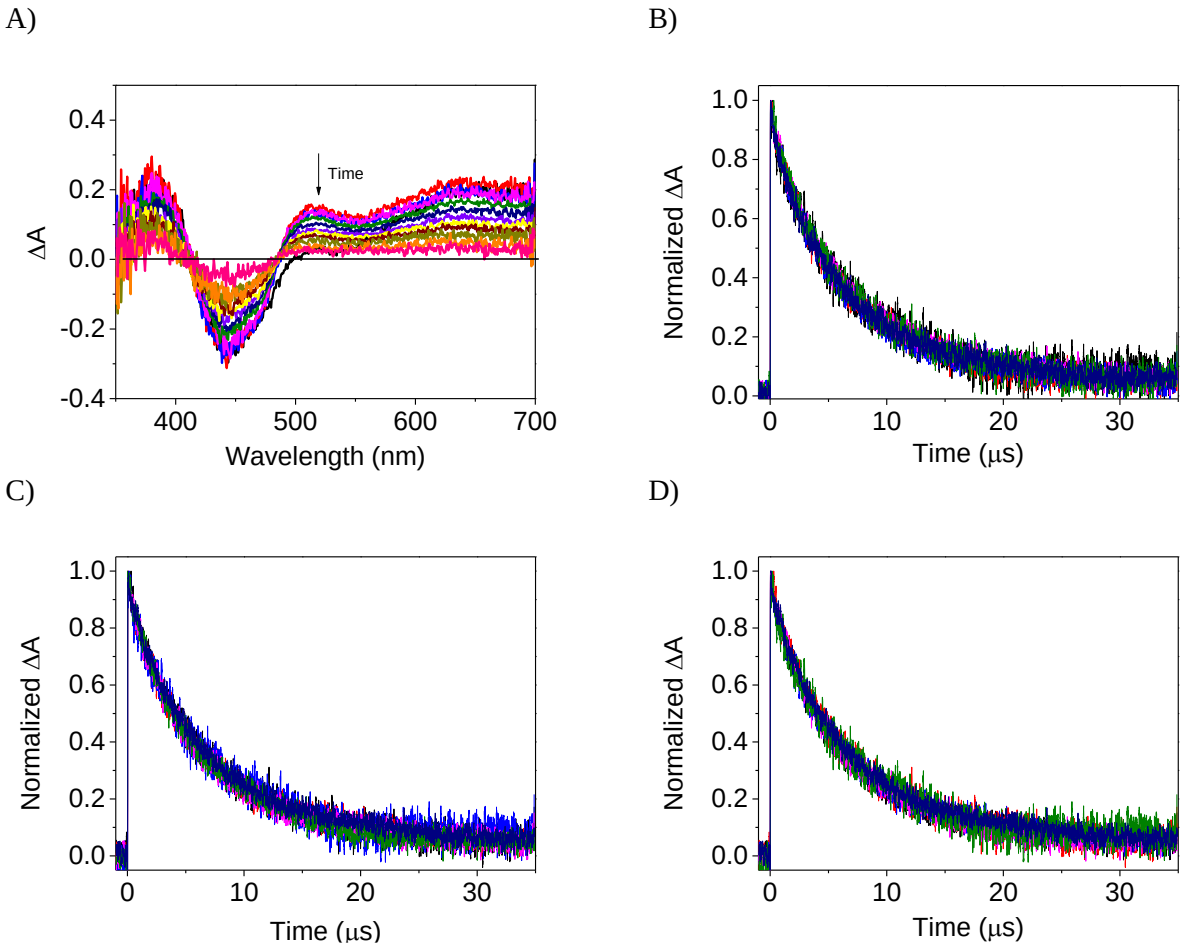

Figure 8. A) Transient spectra of ^{3}RFTA* at different time windows after laser excitation in nitrogen-bubbled acetonitrile (λ_{exc}= 460 nm); decays of ^{3}RFTA* recorded at 620 nm (λ_{exc}= 460 nm) upon increasing concentrations (0-100 μM) of UV-326 (B); UV-327 (C) and UV-328 (D) in deaerated acetonitrile.

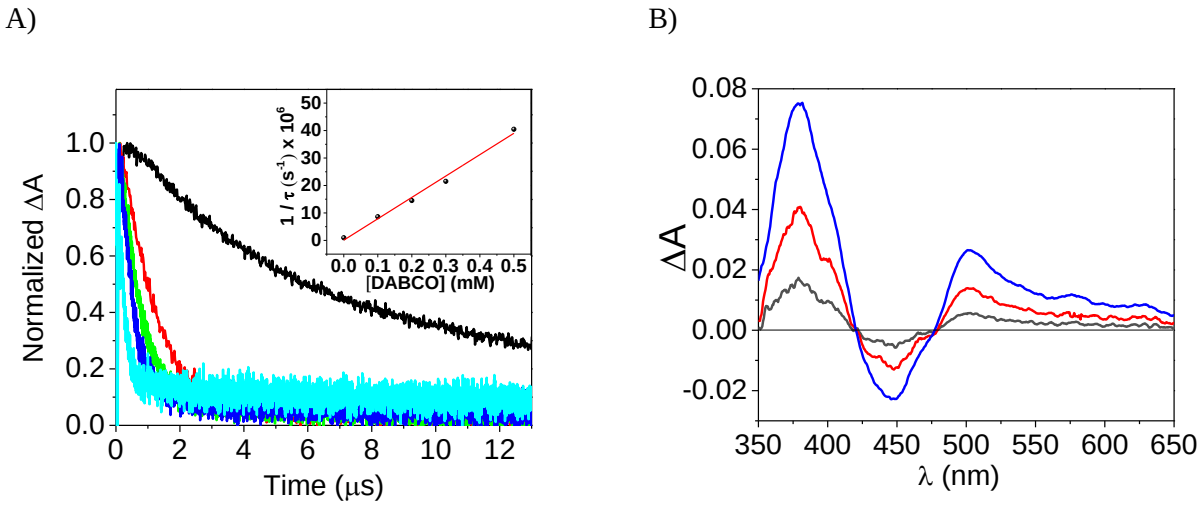

Figure 9. A) Quenching of ^{3}RFTA* upon increasing concentrations of DABCO in deaerated acetonitrile, registered at 620 nm. Inset: corresponding Stern-Volmer plot. B) Transient absorption spectrum of RFTA$^{\bullet-}$ obtained upon laser excitation of RFTA (λ_{exc} = 460 nm) in the presence of DABCO (50 mM).

3.3 Quenching of the reactive intermediates

It is known that ^{3}RFTA* gives rise to the formation of $^1O_2$; in fact, a constant value of k_{qT} = 9.8 x 10^8 $M^{-1}s^{-1}$ has been reported for the quenching of ^{3}RFTA* by O_2.[42] Moreover, having demonstrated that the ^{3}RFTA* also reacts with DABCO giving rise to a second generation of reactive species; the interaction of these species with the filters was studied.

To investigate the interaction of $^1O_2$ with BUVSs, $^1O_2$ was selectively generated upon laser excitation of a Rose Bengal solution in aerated acetonitrile-toluene, at 532 nm, and the decay of its characteristic NIR phosphorescence at 1270 nm was recorded in the presence of increasing concentrations of the BUVSs (Figure 10). In all cases, the emission lifetime slightly decreased with increasing concentrations of BUVSs. The quenching rate constant values obtained upon application of the Stern-Volmer relationships were: k_{q1O2} = 3.3 x 10^5 $M^{-1}s^{-1}$; k_{q1O2} = 3.0 x 10^5 $M^{-1}s^{-1}$ and k_{q1O2} = 3.0 x 10^5 $M^{-1}s^{-1}$, for UV-326, UV-327 and UV-328, respectively.

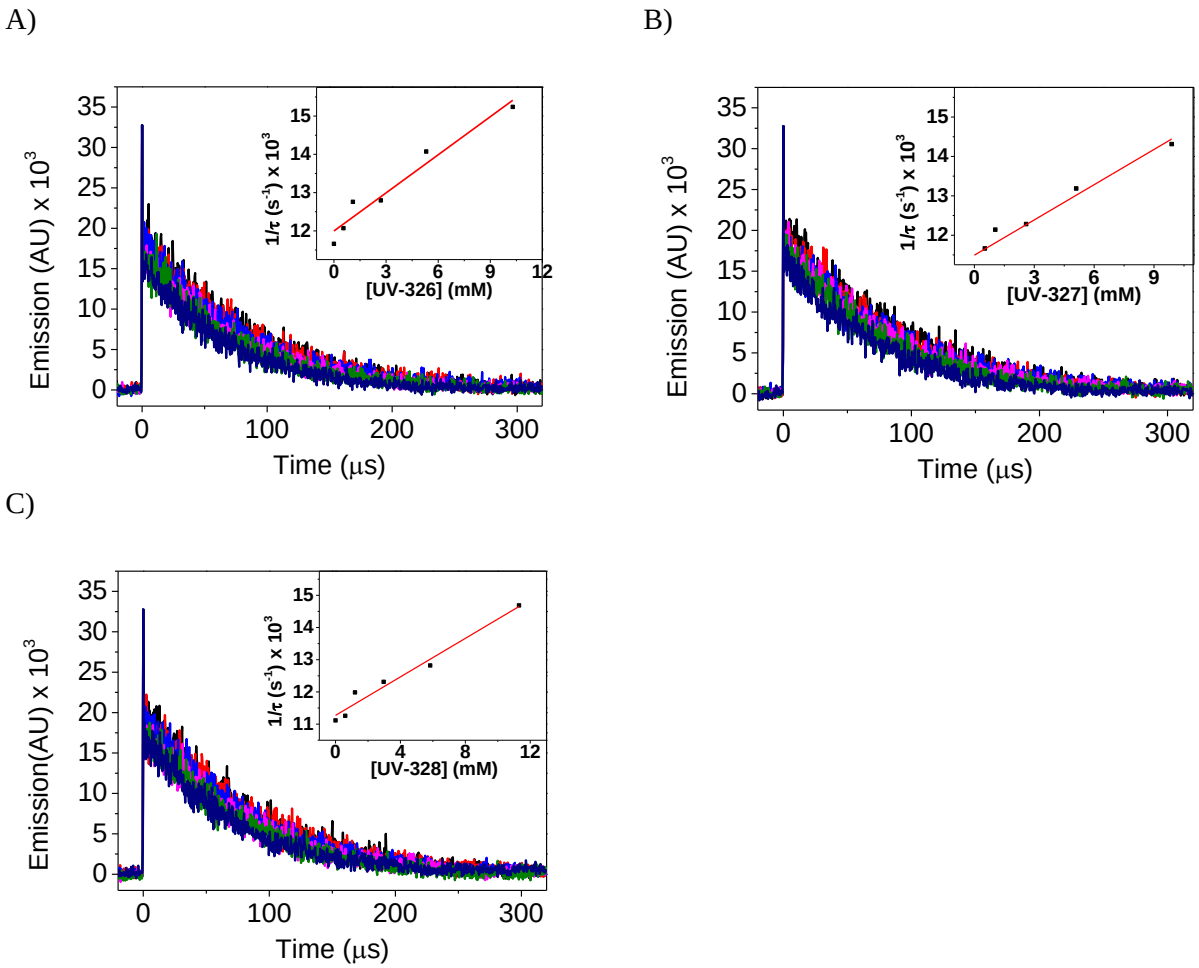

Figure 10. NIR-Phosphorescence decay of $^1O_2$ at 1270 nm after laser excitation of Rose Bengal at 532 nm (Abs $_{532}$ = 0.5), in air-saturated acetonitrile-toluene solutions, upon addition of increasing amounts of UV-326 (A), UV-327 (B) and UV-328 (C). Insets: Stern-Volmer plots.

Finally, deaerated solutions containing RFTA (Abs = 0.3 at the λ_{exc} = 460 nm), DABCO ($5x10^{-2}$ M) and different concentrations of the BUVSs (0-100 μM) were submitted to laser flash photolysis (Figure 11). The

evolution of the generated RFTA$^{\bullet-}$ was monitored at 380 nm. Upon application of the Stern-Volmer relationships, the obtained quenching rate constants values were: k_q = 2.6 x 10^9 $M^{-1}s^{-1}$; k_q = 1.5 x 10^9 $M^{-1}s^{-1}$ and k_q = 6.9 x 10^8 $M^{-1}s^{-1}$, for UV-326, UV-327 and UV-328, respectively.

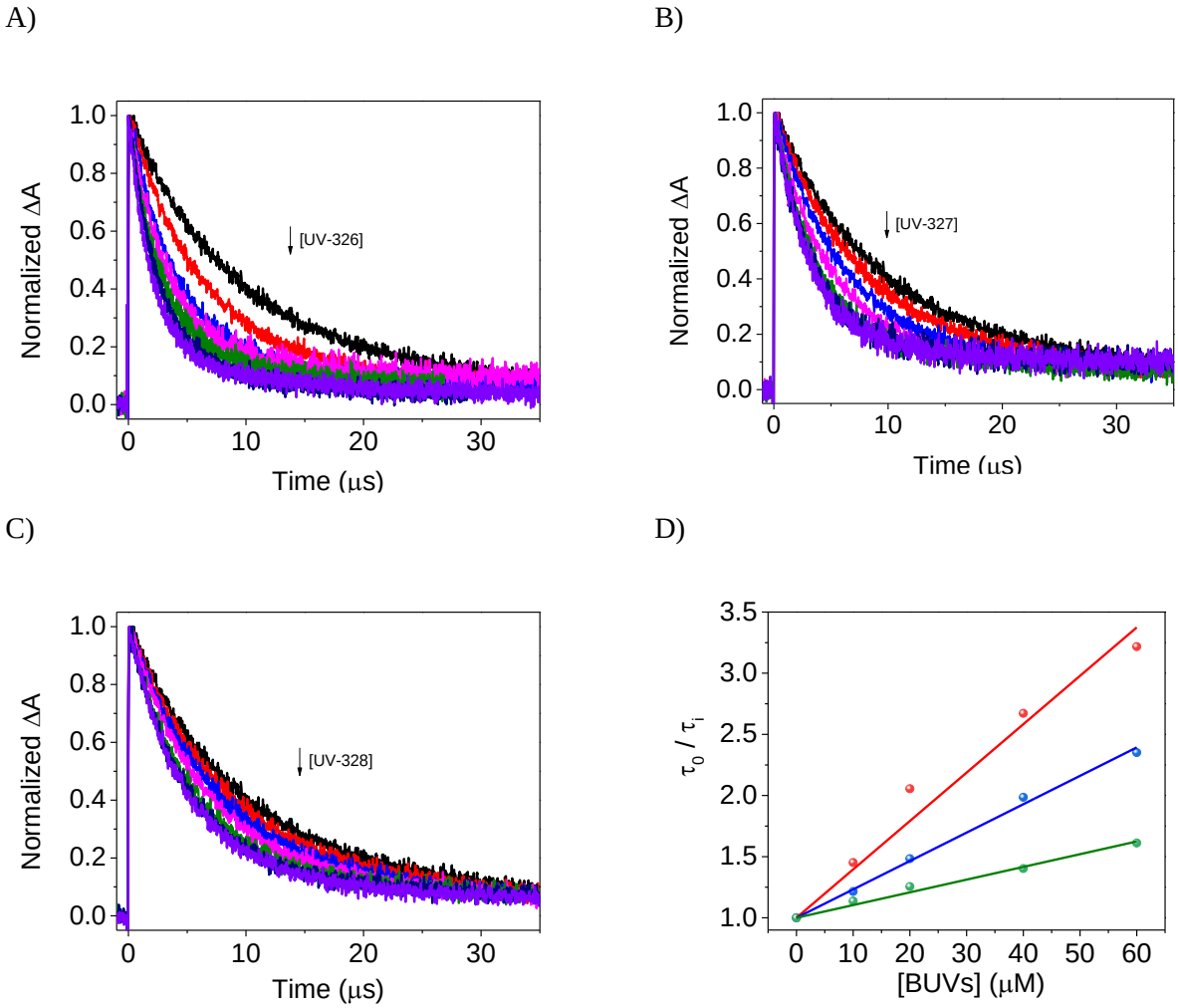

Figure 11. Traces of RFTA$^{\bullet-}$ recorded at 380 nm following laser excitation of deaerated acetonitrile-toluene solutions of RFTA at 460 nm (Abs $_{460}$ = 0.3) in the presence of DABCO (50 mM) and increasing amounts of UV-326 (A), UV-327 (B) and UV-328 (C). Stern-Volmer plots: UV-326 (red), UV-327 (blue) and UV-328 (green) (D).

Discussion

A variety of conditions has been explored to establish the best scenario to produce the abatement of the selected BUVSs. A rigorous investigation of the participation of the excited species directly derived from the absorption of RFTA (singlet and triplet excited states) showed that only DABCO was able to quench efficiently these two excited states (in agreement with thermodynamic calculations, see SI), while (as reported in the literature) oxygen was an efficient triplet quencher in the absence of DABCO. A second generation of reactive species ($^1O_2$ and RFTA$^{\bullet-}$) arose from the reaction between the ^{3}RFTA* and O_2, and $^{1\text{ or }3}$RFTA* with DABCO, respectively. Hence, quenching rate constants for the reaction between the $^1O_2$ and RFTA$^{\bullet-}$ and the BUVSs

were experimentally determined. In a following step, the contribution of each reaction pathway independently tested in the previous section, was evaluated based on the photophysical data of RFTA (see Tables S2 and S3), the determined quenching rate constants (see Table S4) and the experimental BUVSs and DABCO concentrations (1 x 10^{-5} M and 1 x 10^{-2} M, respectively), according to the equations shown in the SI.

On one hand, BUVSs were able to quench the ^{1}RFTA* resulting in the formation of RFTA$^{\bullet-}$, while the ^{3}RFTA* decays without reacting. Nevertheless, when O_2 is present in the media quenching of the ^{3}RFTA* results into the formation of $^{1}O_2$. However, this second-generation reactive species basically decays without being able to oxidize the BUVSs when they are at the operational concentration (10^{-5} M); thus, the observed phtodegradation is only achieved upon long irradiation times (see Figure 4 and Table 1). Nevertheless, the low concentration of radical cations formed by direct interaction of BUVSs with ^{1}RFTA* would react with O_2, which triggers chain reactions increasing the final degradation efficiency. Oxygen would also help to oxidize the RFTA$^{\bullet-}$ to regenerate RFTA closing the catalytic cycle (Scheme 1).

Other authors reported the degradation of the non-chlorinated benzotriazole (BT) assisted by TiO_2 (500 mg/L) using artificial sunlight.[43] Under these conditions, photocatalytic decomposition of BT was achieved after 60 minutes of irradiation at the irradiance equal to 500 W/m^2. As a result of the excitation of TiO_2, hydroxyl radicals are generated, which react indiscriminately with organic contaminants. Although, the results are not easily compared to the ones reported herein since the addressed pollutant is not that recalcitrant, it gives the idea that benzotriazoles are not easily abated under oxidation conditions.

On the other hand, the best results were achieved in the presence of a good e^- donor, such as DABCO. In fact, quenching of $^{1 \text{ or } 3}$RFTA* by DABCO (even in the presence of BUVSs) results in a high percentage of singlets quenched together with a total quenching of the triplets, giving rise to the formation of RFTA$^{\bullet-}$ with *ca*. 70% overall yield, regardless the BUVS or O_2 are present in the media (see Table 2 and thermodynamic calculations in the SI). When the reactivity of RFTA$^{\bullet-}$ is explored, we can observe that still most of this reactive species decays without reacting. Nevertheless, the different percentage of RFTA$^{\bullet-}$ reacting with the BUVs (14.4%, 9.1% and 4.5% for UV-326, UV-327 and UV-328) is in agreement with the observed photodegradation rates and thermodynamic calculations (see Figure 5, Table 2 and SI). An analogous trend was found when water was employed in the calculations instead of acetonitrile (see Table S5 in the SI). Since O_2 was not able to efficiently compete with DABCO for the ^{3}RFTA*, it could participate into the further degradation of the formed BUVSs$^{\bullet-}$, or in the separation of radical cation/radical anion derived from the reaction between DABCO and excited states of RFTA, being participation of the low concentration of $^{1}O_2$ only residual (Scheme 2).

In summary, a deep investigation of the participation of every potential reactive species in scenarios of a gradual level of complexity, together with determination of the quenching rate constants for every reaction pathway, allowed determining that the main reactive species in the photodegradation of BUVSs is RFTA$^{\bullet-}$. On

the basis of the obtained results, plausible mechanisms to explain the observed abatement of the BUVSs in the absence/presence of good e^- donors have been postulated (Scheme 1 and Scheme 2).

Table 1. Relative contribution of the primary and secondary reactive species derived from the visible-light absorption of RFTA in the photodegradation of the BUVSs in aerated acetonitrile solutions.

Reactive species / Quencher	**Quenching of ^{1}RFTA***	**Fluorescence**	**Quenching of ^{3}RFTA***	**Quenching of ^{3}RFTA* by O_2**	**Intrinsic decay of $^1O_2$**	**Quenching of $^1O_2$**
UV-326 (10^{-5} M)	<0.1	53.0	-	45.7	45.7	<0.1
UV-327 (10^{-5} M)	<0.1	53.0	-	45.7	45.7	<0.1
UV-328 (10^{-5} M)	<0.1	53.0	-	45.7	45.7	<0.1

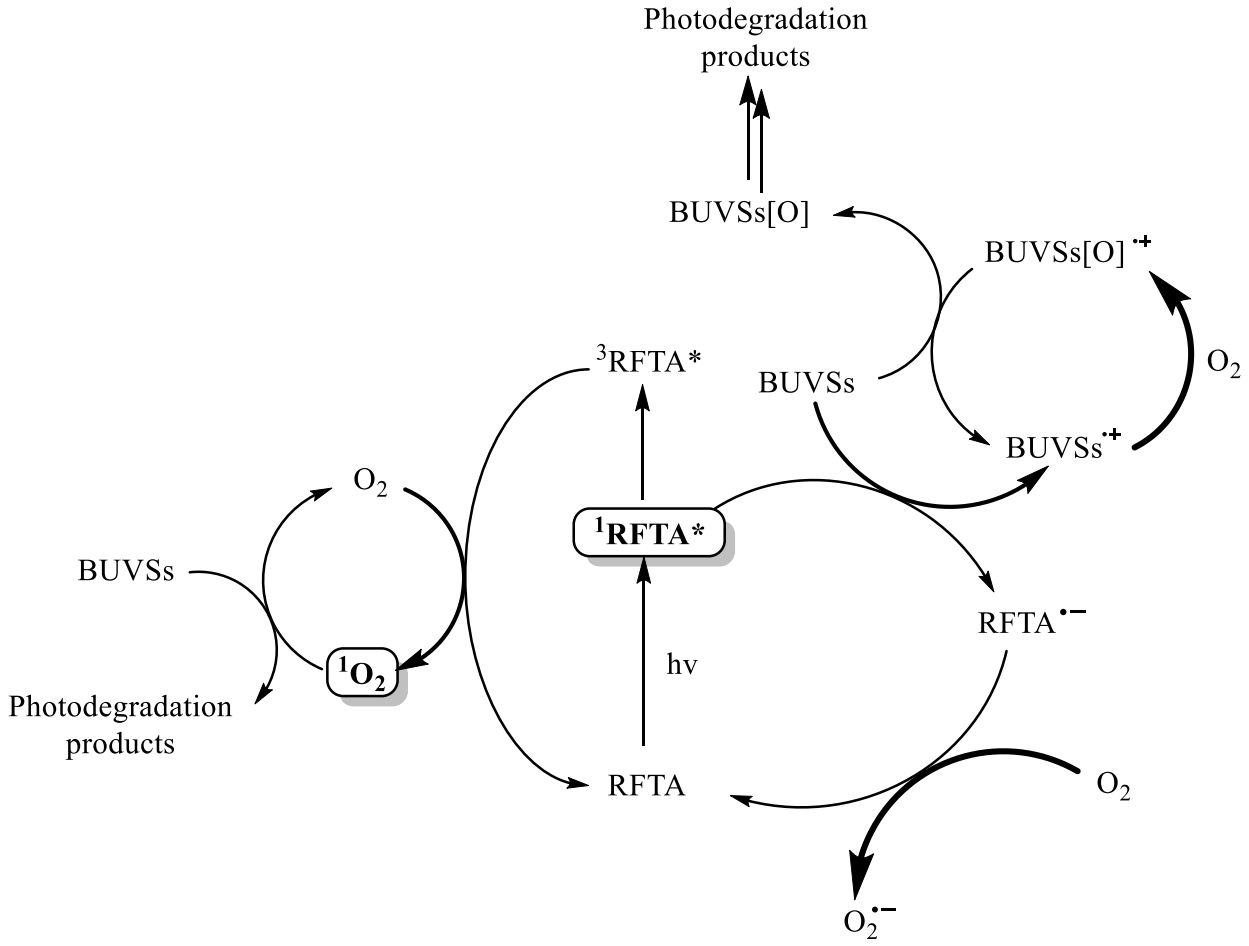

Scheme 1. Photodegradation of BUVSs in the presence of RFTA and O_2, under visible light irradiation.

Table 2. Relative contribution of the primary and secondary reactive species derived from the visible-light absorption of RFTA in the absence/presence of DABCO, in the photodegradation of the BUVSs in aerated acetonitrile solutions.

Reactive species / Quencher	**Quenching of ^{1}RFTA***	**Fluorescence**	**Quenching of ^{3}RFTA***	**Quenching of ^{3}RFTA* by O_2**	**Intrinsic decay of $^1O_2$**	**Quenching of $^1O_2$**	**Intrinsic decay of $RFTA^{\cdot-}$**	**Quenching of $RFTA^{\cdot-}$**
DABCO (10^{-2} M)	47.0	28.1	24.1	0.7	<0.1	0.7	-	-
DABCO (10^{-2} M) + **UV-326** (10^{-5} M)	47.0	28.1	24.1	0.7	<0.1	0.7	56.8	14.4
DABCO (10^{-2} M) + **UV-327** (10^{-5} M)	47.0	28.1	24.1	0.7	<0.1	0.7	62.1	9.1
DABCO (10^{-2} M) + **UV-328** (10^{-5} M)	47.0	28.1	24.1	0.7	<0.1	0.7	66.7	4.5

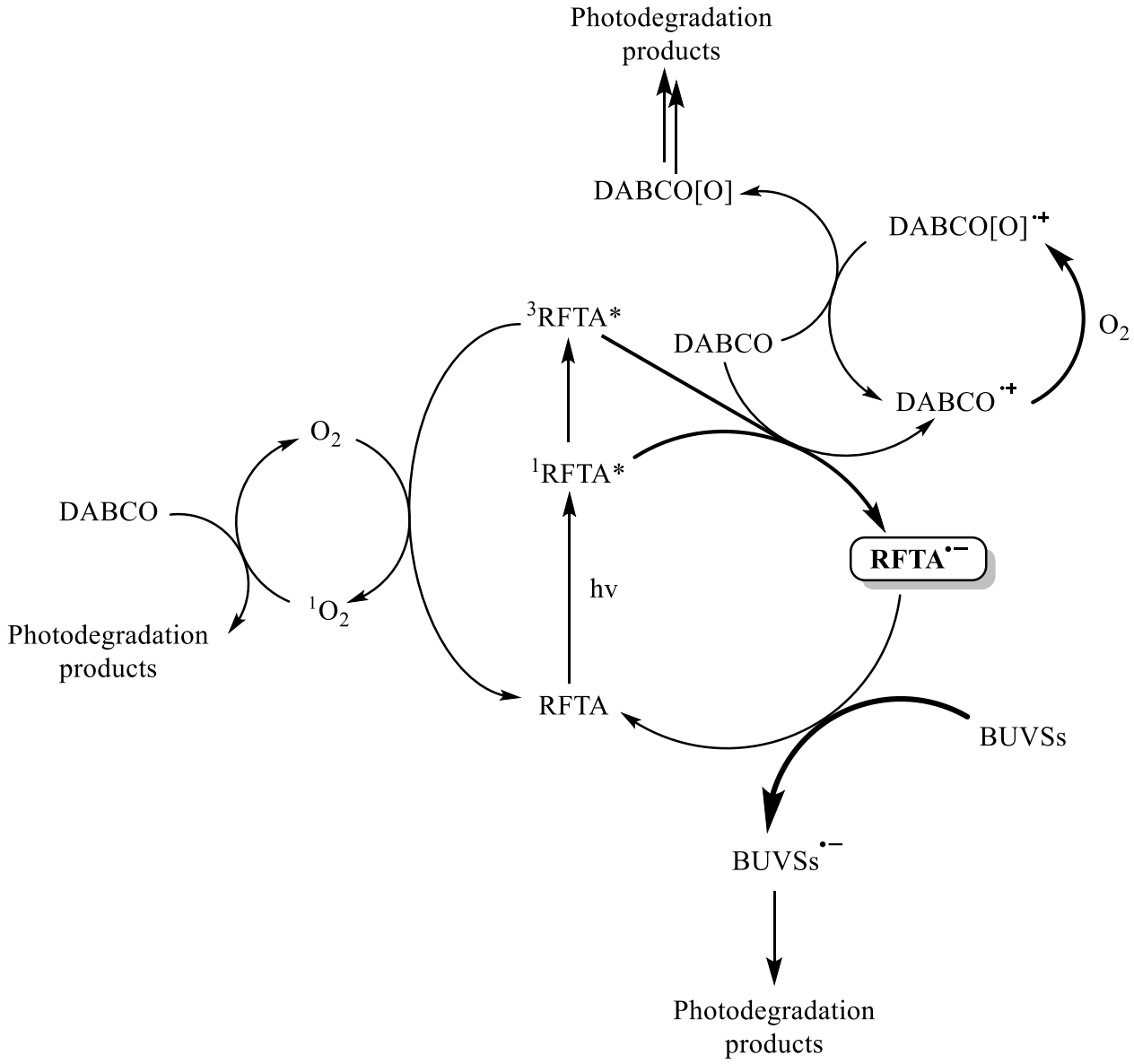

Scheme 2. Photodegradation of BUVSs in the presence of RFTA, DABCO and O_2, under visible light irradiation.

Conclusions

In the present work, the potential of RFTA to achieve the photocatalyzed degradation of recalcitrant pollutants such as benzotriazole derived solar filters (BUVSs) has been experimentally demonstrated. In addition to a moderately efficient oxidative pathway, a much better performing reductive pathway has been found. It involves the use of DABCO as a model sacrificial electron donor, which acts through a massive electron transfer quenching of both the singlet and the triplet excited states of RFTA, to give the radical anion $RFTA^{\bullet-}$. This is the key species that reacts with the solar filters, achieving their reductive abatement from the medium. The participation of O_2 at different stages, such as contributing to separate the radical ions formed enhances

the photodegradation. Thus, we have demonstrated for the first time that the known potential of RFTA as a photocatalyst to produce oxidative degradation of pollutants can be expanded to the photoreduction of more recalcitrant pollutants when RFTA is found in the presence of good electron donors. Even more, a deep understanding on the role of naturally occurring constituents of the environment in the photodegradation of recalcitrant pollutants has been provided. This knowledge would constitute the basis of newer and more sustainable wastewater remediation technologies without the need of additional chemicals in the framework of circular economy.

Funding: This research was funded by H2020/Marie Skłodowska-Curie Actions under the AQUAlity project (Reference: 765860) and European Union's Horizon 2020 research and innovation program under European Research Council (ERC) through the HyMAP project (grant agreement No. 648319). Project PID2019-110441RB-C33 financed by MCIN/AEI/10.13039/501100011033 and AEI-MICINN/FEDER, UE through the Nympha Project (PID2019-106315RB-I00), the regional government of "Comunidad de Madrid" and the European Structural Funds through their financial support to FotoArt-CM project (S2018/NMT-4367) are also acknowledged.

References

[1] S. Weiss, J. Jakobs, T. Reemtsma, Discharge of three benzotriazole corrosion inhibitors with municipal wastewater and improvements by membrane bioreactor treatment and ozonation, Environ. Sci. Technol. 40 (2006) 7193–7199. https://doi.org/10.1021/es061434i.

[2] J.B. Cotton, I.R. Scholes, Benzotriazole and Related ' Compounds As Corrosion Inhibitors for Copper, Brit. Corros. J. 2 (1967) 1–5.

[3] M.G. Cantwell, J.C. Sullivan, R.M. Burgess, Benzotriazoles: History, Environmental Distribution, and Potential Ecological Effects, Elsevier, 2015. https://doi.org/10.1016/B978-0-444-63299-9.00016-8.

[4] H. Nakata, S. Murata, J. Filatreau, Occurrence and Concentrations of Benzotriazole UV Stabilizers in Marine Organisms and Sediments from the Ariake Sea, Japan", Environ. Sci. Technol. 43 (2009) 7999. https://doi.org/10.1021/es902653t.

[5] M.D. Alotaibi, A.J. McKinley, B.M. Patterson, A.Y. Reeder, Benzotriazoles in the Aquatic Environment: A Review of Their Occurrence, Toxicity, Degradation and Analysis, Water. Air. Soil Pollut. 226 (2015). https://doi.org/10.1007/s11270-015-2469-4.

[6] A. Wick, B. Jacobs, U. Kunkel, P. Heininger, T.A. Ternes, Benzotriazole UV stabilizers in sediments, suspended particulate matter and fish of German rivers: New insights into occurrence, time trends and persistency, Environ. Pollut. 212 (2016) 401–412. https://doi.org/10.1016/j.envpol.2016.01.024.

[7] S. Montesdeoca-Esponda, T. Vega-Morales, Z. Sosa-Ferrera, J.J. Santana-Rodríguez, Extraction and

determination methodologies for benzotriazole UV stabilizers in personal-care products in environmental and biological samples, TrAC - Trends Anal. Chem. 51 (2013) 23–32. https://doi.org/10.1016/j.trac.2013.05.012.

[8] Z. Lu, S.A. Smyth, T.E. Peart, A.O. De Silva, Occurrence and fate of substituted diphenylamine antioxidants and benzotriazole UV stabilizers in various Canadian wastewater treatment processes, Water Res. 124 (2017) 158–166. https://doi.org/10.1016/j.watres.2017.07.055.

[9] National Institute of Technology and Evaluation, Japan CHEmicals Collaborative Knowledge database (J-CHECK), (n.d.). https://www.nite.go.jp/chem/jcheck/List6Action?category=211&request_locale=en.

[10] P. Rodríguez-Escales, X. Sanchez-Vila, Modeling the fate of UV filters in subsurface: Co-metabolic degradation and the role of biomass in sorption processes, Water Res. 168 (2020) 115192. https://doi.org/10.1016/j.watres.2019.115192.

[11] K. Fent, G. Chew, J. Li, E. Gomez, Benzotriazole UV-stabilizers and benzotriazole: Antiandrogenic activity in vitro and activation of aryl hydrocarbon receptor pathway in zebrafish eleuthero-embryos, Sci. Total Environ. 482–483 (2014) 125–136. https://doi.org/10.1016/j.scitotenv.2014.02.109.

[12] H. Nagayoshi, K. Kakimoto, S. Takagi, Y. Konishi, K. Kajimura, T. Matsuda, Benzotriazole ultraviolet stabilizers show potent activities as human aryl hydrocarbon receptor ligands, Environ. Sci. Technol. 49 (2015) 578–587. https://doi.org/10.1021/es503926w.

[13] S. Zhang, J. Wang, Y. Zhang, J. Ma, L. Huang, S. Yu, L. Chen, G. Song, M. Qiu, X. Wang, Applications of water-stable metal-organic frameworks in the removal of water pollutants: A review, Environ. Pollut. 291 (2021) 118076. https://doi.org/10.1016/j.envpol.2021.118076.

[14] S. Yu, H. Pang, S. Huang, H. Tang, S. Wang, M. Qiu, Z. Chen, H. Yang, G. Song, D. Fu, B. Hu, X. Wang, Recent advances in metal-organic framework membranes for water treatment: A review, Sci. Total Environ. 800 (2021) 149662. https://doi.org/10.1016/j.scitotenv.2021.149662.

[15] Y. Zou, Y. Hu, Z. Shen, L. Yao, D. Tang, S. Zhang, S. Wang, B. Hu, G. Zhao, X. Wang, Application of aluminosilicate clay mineral-based composites in photocatalysis, J. Environ. Sci. (China). 115 (2022) 190–214. https://doi.org/10.1016/j.jes.2021.07.015.

[16] G. Sharma, A. Kumar, M. Naushad, B. Thakur, D.V.N. Vo, B. Gao, A.A. Al-Kahtani, F.J. Stadler, Adsorptional-photocatalytic removal of fast sulphon black dye by using chitin-cl-poly(itaconic acid-co-acrylamide)/zirconium tungstate nanocomposite hydrogel, J. Hazard. Mater. 416 (2021) 125714. https://doi.org/10.1016/j.jhazmat.2021.125714.

[17] Z. Fallah, E.N. Zare, M. Ghomi, F. Ahmadijokani, M. Amini, M. Tajbakhsh, M. Arjmand, G. Sharma, H. Ali, A. Ahmad, P. Makvandi, E. Lichtfouse, M. Sillanpää, R.S. Varma, Toxicity and

remediation of pharmaceuticals and pesticides using metal oxides and carbon nanomaterials, Chemosphere. 275 (2021) 130055. https://doi.org/10.1016/j.chemosphere.2021.130055.

[18] M. Qiu, B. Hu, Z. Chen, H. Yang, L. Zhuang, X. Wang, Challenges of organic pollutant photocatalysis by biochar-based catalysts, Biochar. 3 (2021) 117–123. https://doi.org/10.1007/s42773-021-00098-y.

[19] A. Bétard, R.A. Fischer, Metal-organic framework thin films: From fundamentals to applications, Chem. Rev. 112 (2012) 1055–1083. https://doi.org/10.1021/cr200167v.

[20] M. Kadhom, B. Deng, Metal-organic frameworks (MOFs) in water filtration membranes for desalination and other applications, Appl. Mater. Today. 11 (2018) 219–230. https://doi.org/10.1016/j.apmt.2018.02.008.

[21] K. McNeill, S. Canonica, Triplet state dissolved organic matter in aquatic photochemistry: Reaction mechanisms, substrate scope, and photophysical properties, Environ. Sci. Process. Impacts. 18 (2016) 1381–1399. https://doi.org/10.1039/c6em00408c.

[22] X. Chen, J. Wang, J. Chen, C. Zhou, F. Cui, G. Sun, Photodegradation of 2-(2-hydroxy-5-methylphenyl)benzotriazole (UV-P) in coastal seawaters: Important role of DOM, J. Environ. Sci. (China). 85 (2019) 129–137. https://doi.org/10.1016/j.jes.2019.05.017.

[23] J.P. Escalada, A. Pajares, J. Gianotti, A. Biasutti, S. Criado, P. Molina, W. Massad, F. Amat-Guerri, N.A. García, Photosensitized degradation in water of the phenolic pesticides bromoxynil and dichlorophen in the presence of riboflavin, as a model of their natural photodecomposition in the environment, J. Hazard. Mater. 186 (2011) 466–472. https://doi.org/10.1016/j.jhazmat.2010.11.026.

[24] A. Pavanello, D. Fabbri, P. Calza, D. Battiston, M.A. Miranda, M.L. Marin, Photocatalytic degradation of drugs in water mediated by acetylated riboflavin and visible light: A mechanistic study, J. Photochem. Photobiol. B Biol. 221 (2021) 112250. https://doi.org/10.1016/j.jphotobiol.2021.112250.

[25] A. Pavanello, D. Fabbri, P. Calza, D. Battiston, M.A. Miranda, M.L. Marin, Biomimetic Photooxidation of Noscapine Sensitized by a Riboflavin Derivative in Water: the Combined Role of Natural Dyes and Solar Light in Environmental Remediation, J. Photochem. Photobiol. B Biol. 229 (2022). https://doi.org/https://doi.org/10.1016/j.jphotobiol.2022.112415.

[26] P.F. Heelis, The photophysical and photochemical properties of flavins (isoalloxazines), Chem. Soc. Rev. 11 (1982) 15–39. https://doi.org/10.1039/CS9821100015.

[27] S.G. Bertolotti, C.M. Previtali, A.M. Rufs, M. V. Encinas, Riboflavin/triethanolamine as photoinitiator system of vinyl polymerization. A mechanistic study by laser flash photolysis, Macromolecules. 32 (1999) 2920–2924. https://doi.org/10.1021/ma981246f.

[28] G. Porcal, S.G. Bertolotti, C.M. Previtali, M. V. Encinas, Electron transfer quenching of singlet and triplet excited states of flavins and lumichrome by aromatic and aliphatic electron donors, Phys. Chem. Chem. Phys. 5 (2003) 4123–4128. https://doi.org/10.1039/b306945a.

[29] W. Chen, J.J. Chen, R. Lu, C. Qian, W.W. Li, H.Q. Yu, Redox reaction characteristics of riboflavin: A fluorescence spectroelectrochemical analysis and density functional theory calculation, Bioelectrochemistry. 98 (2014) 103–108. https://doi.org/10.1016/j.bioelechem.2014.03.010.

[30] S.L.J. Tan, R.D. Webster, Electrochemically induced chemically reversible proton-coupled electron transfer reactions of riboflavin (Vitamin B 2), J. Am. Chem. Soc. 134 (2012) 5954–5964. https://doi.org/10.1021/ja300191u.

[31] A. Masek, E. Chrzescijanska, M. Zaborski, M. MacIejewska, Characterisation of the antioxidant acitivity of riboflavin in an elastomeric composite, Comptes Rendus Chim. 15 (2012) 524–529. https://doi.org/10.1016/j.crci.2012.01.012.

[32] J. Meng, F. Xu, S. Yuan, Y. Mu, W. Wang, Z.H. Hu, Photocatalytic oxidation of roxarsone using riboflavin-derivative as a photosensitizer, Chem. Eng. J. 355 (2019) 130–136. https://doi.org/10.1016/j.cej.2018.08.127.

[33] C.K. Remucal, K. McNeill, Photosensitized amino acid degradation in the presence of riboflavin and its derivatives, Environ. Sci. Technol. 45 (2011) 5230–5237. https://doi.org/10.1021/es200411a.

[34] R.A. Larson, P.L. Stackhouse, T.O. Crowley, Riboflavin Tetraacetate: A Potentially Useful Photosensitizing Agent for the Treatment of Contaminated Waters, Environ. Sci. Technol. 26 (1992) 1792–1798. https://doi.org/10.1021/es00033a013.

[35] J.Y. Liang, J.M.P. Yuann, Z.J. Hsie, S.T. Huang, C.C. Chen, Blue light induced free radicals from riboflavin in degradation of crystal violet by microbial viability evaluation, J. Photochem. Photobiol. B Biol. 174 (2017) 355–363. https://doi.org/10.1016/j.jphotobiol.2017.08.018.

[36] W. Massad, S. Criado, S. Bertolotti, A. Pajares, J. Gianotti, J.P. Escalada, F. Amat-Guerri, N.A. García, Photodegradation of the herbicide Norflurazon sensitised by Riboflavin. A kinetic and mechanistic study, Chemosphere. 57 (2004) 455–461. https://doi.org/10.1016/j.chemosphere.2004.06.021.

[37] R. Martinez-Haya, M.A. Miranda, M.L. Marin, Metal-Free Photocatalytic Reductive Dehalogenation Using Visible-Light: A Time-Resolved Mechanistic Study, European J. Org. Chem. 2017 (2017) 2164–2169. https://doi.org/10.1002/ejoc.201601494.

[38] B.P. Vellanki, B. Batchelor, A. Abdel-Wahab, Advanced reduction processes: A new class of treatment processes, Environ. Eng. Sci. 30 (2013) 264–271. https://doi.org/10.1089/ees.2012.0273.

[39] J. Cui, P. Gao, Y. Deng, Destruction of Per- A nd Polyfluoroalkyl Substances (PFAS) with Advanced

Reduction Processes (ARPs): A Critical Review, Environ. Sci. Technol. 54 (2020) 3752–3766. https://doi.org/10.1021/acs.est.9b05565.

[40] D.U. Mccormick, Flavin Derivatives via Bromination of the 8-Methyl Substituent (1), J. Heterocycl. Chem. 7 (1970) 447–450. https://doi.org/10.1002/jhet.5570070240C.

[41] S.L. Murov, I. Carmichael, G.L. Hug, Handbook of Photochemistry, 2nd ed., Marcel Dekker, New York, 2009.

[42] D.R. Cardoso, S.H. Libardi, L.H. Skibsted, Riboflavin as a photosensitizer. Effects on human health and food quality, Food Funct. 3 (2012) 487–502. https://doi.org/10.1039/c2fo10246c.

[43] E. Felis, A. Sochacki, S. Magiera, Degradation of benzotriazole and benzothiazole in treatment wetlands and by artificial sunlight, Water Res. 104 (2016) 441–448. https://doi.org/10.1016/j.watres.2016.08.037.